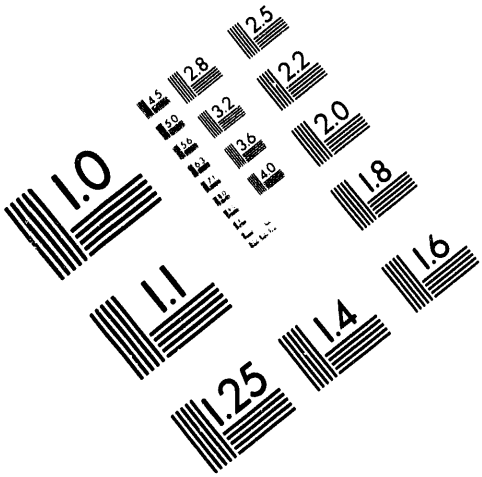

Association for Information and Image Management

1100 Wayne Avenue, Suite 1100
Silver Spring, Maryland 20910

301/587-8202

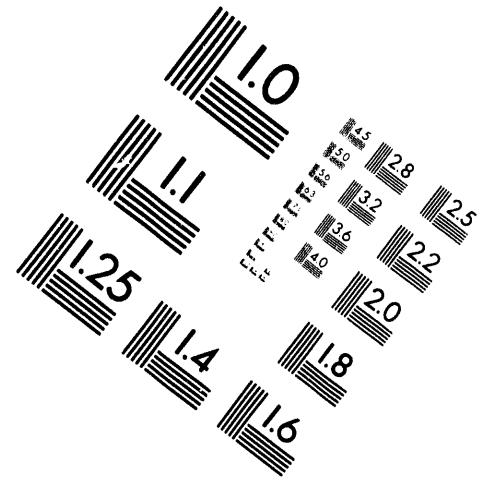

Centimeter

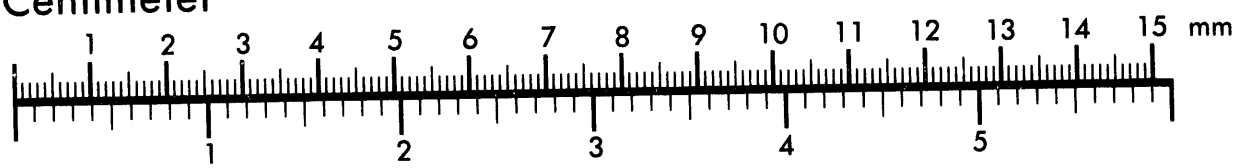

Inches

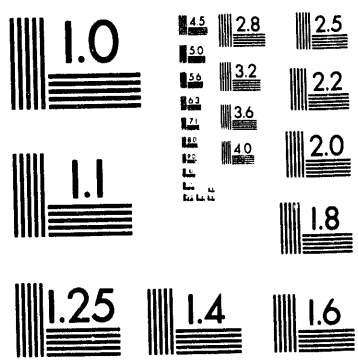

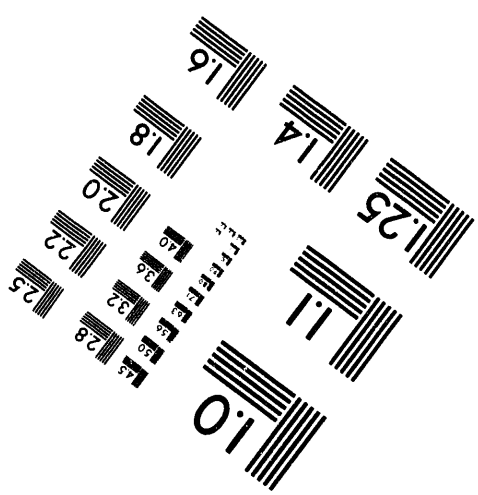

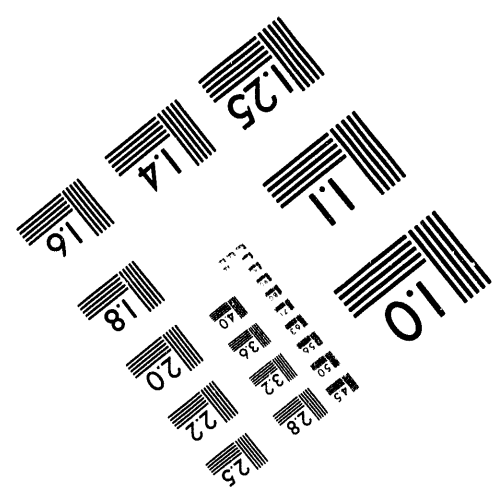

MANUFACTURED TO AIIM STANDARDS
BY APPLIED IMAGE, INC.

1 of 1

Conf-921101--143

RAMAN SPECTROSCOPY OF C-IRRADIATED GRAPHITE*

D.M. HEMBREE, JR.[1], D.F. PEDRAZA[2], G.R. ROMANOSKI[2], S.P. WITHROW[2] and B.K. ANNIS[2]

[1]Oak Ridge Y-12 Plant, Oak Ridge, TN 37831
[2]Oak Ridge National Laboratory, Oak Ridge, TN 37831

ABSTRACT

Highly oriented pyrolytic graphite samples were irradiated with C^+ ions at 35 keV in a direction normal to the basal plane and subsequently annealed up to 1373 K. Substantial surface topography changes were observed at fluences of $5x10^{18}$ ions/m^2 and higher using scanning electron and atomic force microscopies. Intricate networks of surface cracks and ridges developed after high dose implantation. A systematic study of the irradiation effects was conducted using Raman spectroscopy. Microstructural changes in irradiated regions were first detected at a dose of $1x10^{17}$ ions/m^2 through the appearance of the Raman D-line at ~1360 cm^{-1}. The intensity of this line increases while that of the Raman G-line at 1580 cm^{-1} decreases as the irradiation dose is increased or the irradiation temperature is decreased. After irradiation at 280K to a fluence of $5x10^{19}$ ions/m^2 or higher the first order spectrum exhibits one single line at a wavelength intermediate between the D- and G-lines. Damage recovery upon thermal annealing depends not only on the initial damage state but also on the annealing temperature sequence. Samples irradiated to a damage level where two distinct Raman peaks are no longer resolvable exhibited upon direct annealing at a high temperature two distinct Raman lines. By contrast, pre-annealing these highly irradiated specimens at lower temperatures produced less pronounced changes in the Raman spectra. Pre-annealing appears to stabilize damage structures that are more resistant to high-temperature annealing than those induced by irradiation.

MASTER

INTRODUCTION

Raman spectroscopy has been used extensively to characterize the degree of crystalline perfection of graphite since the pioneering work of Tuinstra and Koenig [1]. The Raman spectrum of pristine single crystal graphite exhibits a single Lorentzian-shaped first order line (the G-line) at 1580 cm^{-1} assigned to the E_{2g} C-C stretching mode. For polycrystalline graphite another line (the D-line) appears near 1355 cm^{-1}. This line has been attributed to scattering from an A_{1g} mode that becomes active because of a breakdown of the wavevector selection rule as a result of finite crystal size effects [1]. The intensity ratio of these two lines I_D/I_G, has been successfully correlated with the inverse in-plane correlation length obtained from x-ray data for different graphites [1].

The submitted manuscript has been authored by a contractor of the U.S. Government under contract No. DE-AC05-84OR21400. Accordingly, the U.S. Government retains a nonexclusive, royalty-free license to publish or reproduce the published form of this contribution, or allow others to do so, for U.S. Government

DISTRIBUTION OF THIS DOCUMENT IS UNLIMITED

In radiation-damaged graphite, the changes of both first and second order Raman spectra observed at increasing doses are fairly complex [2-5]. As the ion irradiation dose is increased, the intensity of the D-line increases while the intensity of the G-line decreases, and second order peaks at ~2725 and 3250 cm^{-1} gradually disappear [2]. Also, the first order peak positions shift and finally merge into a single asymmetric line which has been related to amorphization of the damaged region [2-5].

The effects of implantation temperature and of post-implantation annealing have also been investigated during the last decade [6,7]. Damage recovery has been observed to start at fairly low temperatures, depending on both implantation temperature and fluence. For instance, the Raman line intensity ratio, I_D/I_G, of graphite implanted at 523 K with B to 2.8×10^{19} ions/m^2 is observed to decrease by annealing at temperatures as low as 523 K. For graphite implanted to the same B dose but at 300 K, the decrease in the ratio starts after ~700 K [6]. It has been pointed out that the use of the Tuinstra and Koenig relationship [1] between Raman band intensities and crystallite size leads to the conclusion that crystallite size growth occurs at temperatures much lower than expected for un-irradiated imperfect graphite [7].

It is apparent from work published in the open literature (e.g., references 1 to 3) that changes in the Raman spectra of single crystalline or highly oriented pyrolytic graphite (HOPG) that have been subjected to different levels of irradiation damage could have an origin quite different from differences observed between other imperfect graphites, such as charcoal, carbon blacks, turbostratic and vitreous carbons [8]. In this work, we have performed a systematic study of C-irradiation effects in HOPG as observed by Raman spectroscopy. The influence of irradiation temperature and dose were investigated, as well as the effects of post-irradiation thermal annealing up to 1373 K.

After ion irradiation, topography changes have been reported which become important at higher fluences ϕ_t, e.g., $\phi_t > 1 \times 10^{19}$ ions/m^2, for P- and As-ion bombardment at 100 keV [1]. We have also observed and characterized these types of changes under C-irradiation at 35 and 165 keV. A complete report of the topography changes is given in detail elsewhere [9].

EXPERIMENTAL PROCEDURE

Highly oriented pyrolytic graphite with a c-axis scatter less than 0.5° was cleaved with scotch tape producing specimens ~50 μm thick. The specimens were implanted at 280 K with 35 keV C^+ ions to fluences between 1×10^{16} and 5×10^{21} ions/m^2. The flux was 5.1×10^{16} ions/m^2s. Some higher dose implantations (5×10^{18}, 5×10^{19} and 5×10^{21} ions/m^2) were carried out at 575 K and 873 K as well. The pressure in the implantation chamber was kept below 1×10^{-6} torr.

Thermal anneals were carried out in a vacuum better than 1×10^{-5} torr. Stepwise 1-h anneals were performed at 873, 1023, 1173, 1273 and

1373 K. These were preceded by two 4-h anneals each, at 673 K and 773 K. Other implanted specimens were annealed directly at 1273 K for 2 h.

Optical and scanning electron microscopy (SEM) were used to observe the as-implanted surfaces. Scanning tunneling microscopy (STM) and atomic force microscopy (AFM) were used to quantitatively characterize the changes that occurred in the surface topography at high irradiation doses.

Raman spectra were acquired at room temperature using an Instruments SA Model U1000 spectrometer equipped with a Nachet microscope. The 514.532-nm line from a Coherent Innova 90-5 argon ion laser served as the excitation source.

RESULTS AND DISCUSSION

Surface Topography Changes

High-dose, low-temperature implantation produces substantial alterations of the surface topography of ion-implanted graphite. Figure 1 is an optical micrograph of a specimen irradiated at 280 K to a fluence of 5×10^{19} ions/m^2. A dendrite-like network of channels can be seen. These channels are cracks in the surface, as confirmed by SEM (Fig. 2). A much finer network of curvilinear features is barely visible in Fig. 1, but appears much clearer in Fig. 2. These features were profiled by AFM in samples irradiated to 9×10^{18} ions/m^2 and found to be ridges with heights varying between 4 and 20 nm and widths of 0.1 to 0.2 μm. The cracks were found to have widths on the order of 1 μm and depths of about 250 nm (about three times the calculated ion range). Fig. 3 illustrates the topographical features of an implanted specimen as seen by AFM. At higher implantation temperatures, the surface features tend to be absent,

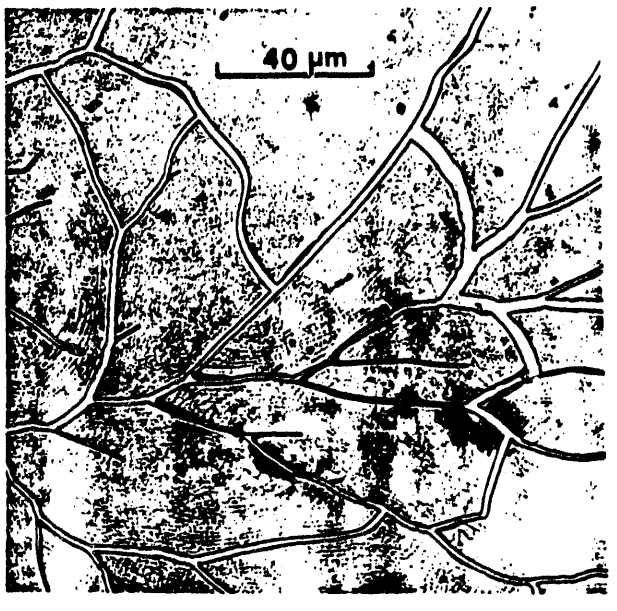

Figure 1. Optical micrograph of a sample irradiated at 280 K to a fluence of 5×10^{19} ions/m^2 showing a dendritic crack network.

Figure 2. SEM image of a region of the specimen shown in Fig. 1. Notice the large crack and the intricate network of surface features.

especially the cracks. Ridges can still be observed as shown in Fig. 4. No indication of order at the atomic level was found by AFM. Small patches showing atomic rows were occasionally observed by STM.

Graphite crystals are known to undergo dimensional changes under irradiation [10]. They expand in a direction parallel to the c-crystallographic axis, and contract in all directions parallel to the basal

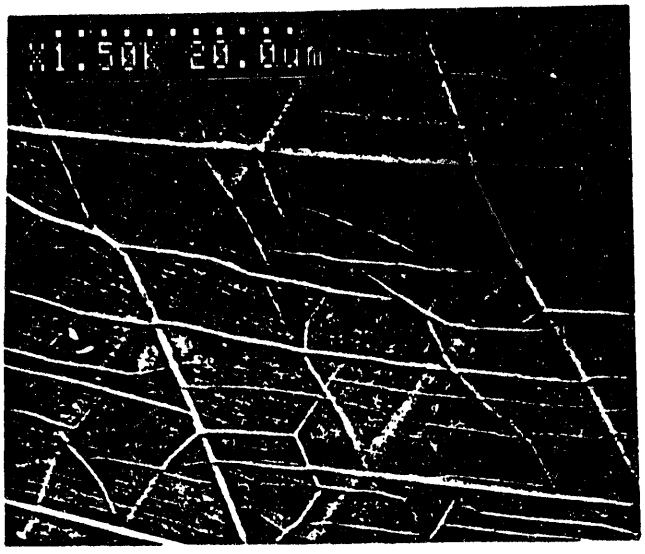

Figure 3. SEM image of a sample irradiated at 573 K to a fluence of $5x10^{19}$ ions/m^2 .

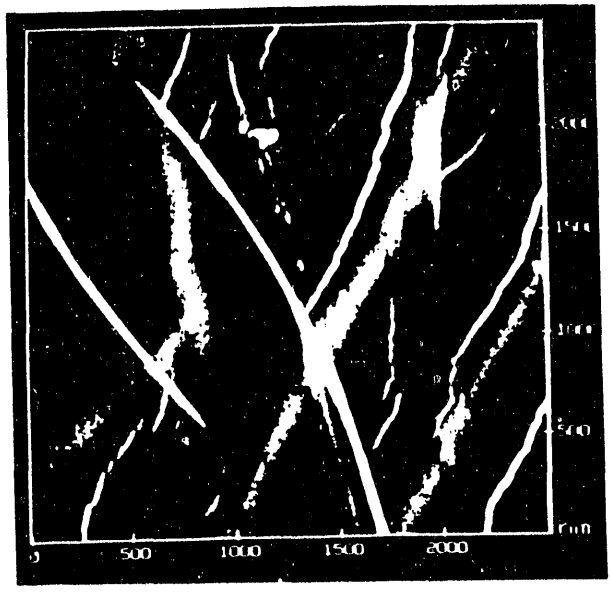

Figure 4. AFM image from a sample implanted at 280 K to a fluence of $9x10^{18}$ ions/m^2, demonstrating that the networks seen in Figs. 2 and 3 are ridges.

plane. This irradiation-induced dimensional change at constant volume is known as irradiation growth. Under ion bombardment, contraction parallel to the irradiated surface only occurs in the damaged thin surface layer. A large shearing stress develops between this layer and the underlying undamaged material, causing the surface cracking. Ridges appear to originate as a result of radiation damage as well. Under irradiation, the damaged basal planes break up into small fragments that are rotated relative to a direction in the original undamaged plane [11]. This fragmentation leaves spacings that could become fast diffusion paths for irradiation-induced interstitials; a fraction of them migrating to the surface can build up the observed ridges [9].

Raman Spectroscopy Studies

The damaged region of graphite bombarded with C-ions at 35 keV extends to a calculated depth of ~100 nm, with the peak damage depth of ~60 nm and an ion range of 83 nm, as calculated using the TRIM code [12]. At a fluence of $3.85x10^{19}$ ions/m^2, the implanted C amounts to one atomic layer. Raman spectra were taken well away from the surface cracks described above. Since the optical skin depth for the 514.5-nm argon ion laser light is ~ 40 nm (well below the ion range), the spectra

arise from the damaged region only, with possible minor contributions from the ridge structures.

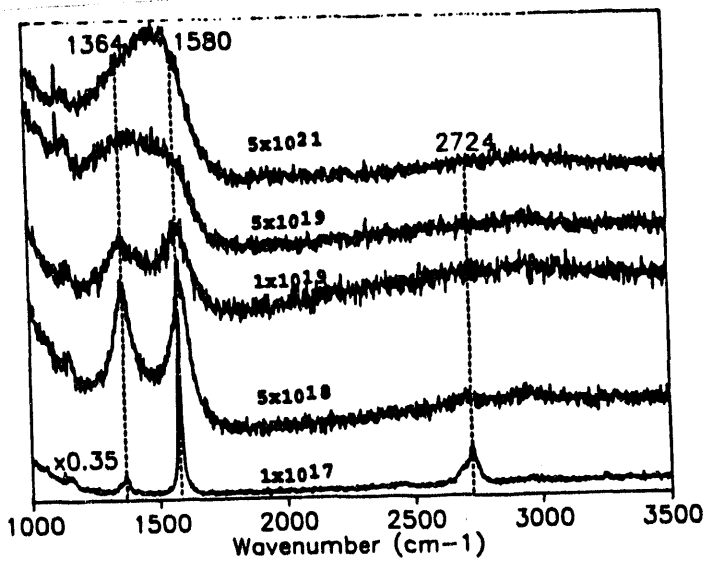

Figure 5. Fluence dependence of Raman spectra of highly oriented pyrolytic graphite implanted at room temperature. Fluence units are ions/m^2.

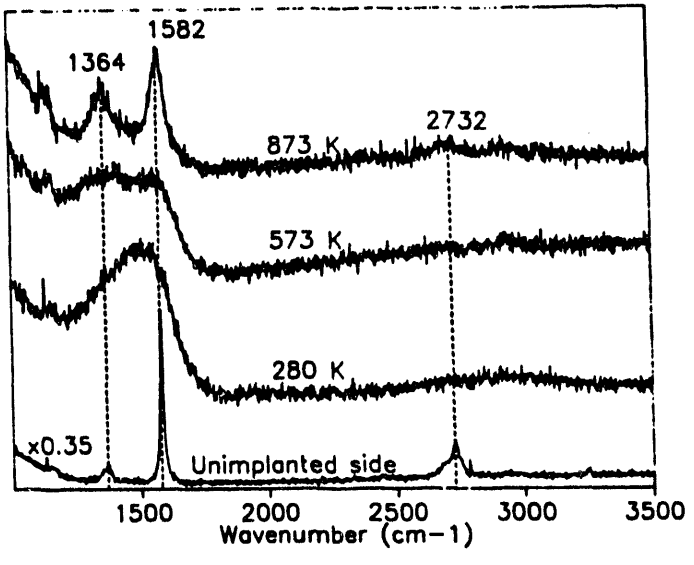

Figure 6. Effect of implantation temperature on Raman spectra of highly oriented pyrolytic graphite implanted to $5x10^{21}$ ions/m^2.

Figure 5 illustrates the fluence dependence of the Raman spectra for implantations carried out at room temperature. Implantation at the lowest fluence, $1x10^{16}$ ions/m^2, produced no changes in the Raman spectrum of graphite. After exposure to $1x10^{17}$ ions/m^2 the 1355 cm^{-1} line appeared at low intensity. It can be seen that as the dose is increased the intensity of the D-line increases relative to that of the G-line, while both lines broaden. At fluences higher than ~$1.7x10^{19}$ ions/m^2 the two lines begin shifting toward each other and start merging. At $5x10^{19}$ ions/m^2 two distinct lines are no longer resolved with the shape of the single line exhibiting a skewness toward the higher wavenumbers. As expected, the Raman spectra of the unimplanted side of the samples were characteristic of pristine graphite, with no observable D-line. However, there were two exceptions, viz., the samples implanted to the highest dose, $5x10^{21}$ ions/m^2, which exhibited a low intensity D-line for the 280 K implantation and an incipient D feature for the 573 K implantation. Fig. 6 shows the implantation temperature dependence of the Raman spectra, illustrated here for the highest dose, $5x10^{21}$ ions/m^2. The effect is very large. For the 573 K implantation, the spectrum is comparable to that of the specimen implanted at 280 K to a fluence of $5x10^{19}$ ions/m^2, while for the 873 K implantation the effect is similar to the 280 K implant at a fluence 3 orders of magnitude lower, i.e.,

5×10^{18} ions/m^2. Assuming that the damage-induced microstructure is the same in this implantation temperature range and that interstitial diffusion controls this microstructure, an activation energy can be calculated using the relation

$$\ln \frac{\phi_1}{\phi_2} = \frac{Q}{k} \left(\frac{1}{T_2} - \frac{1}{T_1} \right)$$

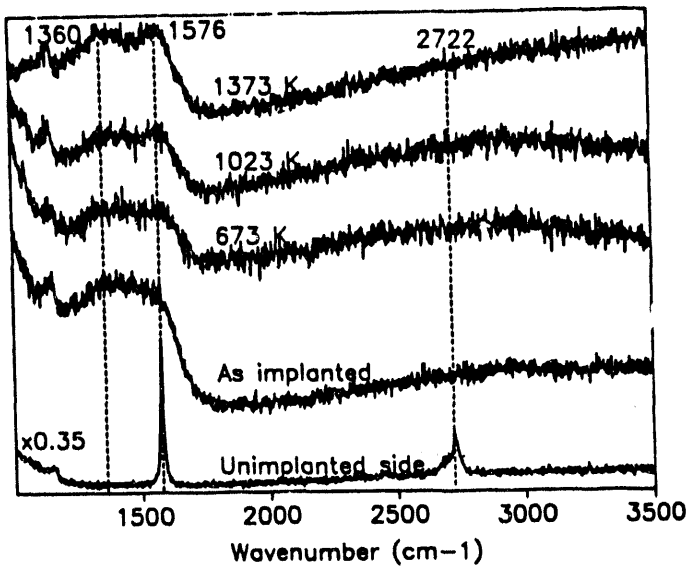

Figure 7. Effect of stepwise, post-implantation thermal annealing on Raman spectra of HOPG implanted to 5×10^{19} ions/m^2 at room temperature. Specimen was annealed for 4 hours at 573 and 673K and 1 hour at each higher temperature.

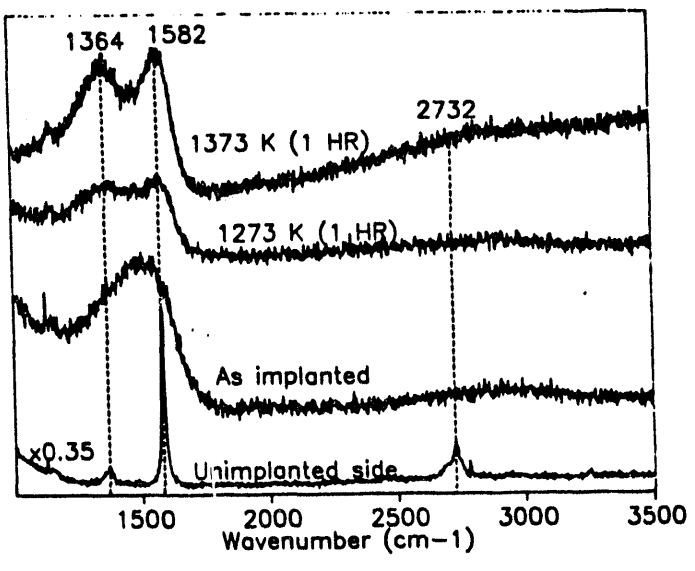

Figure 8. Raman spectra illustrating the effect of directly annealing HOPG at high temperature. Samples were implanted to 5×10^{21} ions/m^2 at room temperature.

where Q is the activation energy for diffusion, and ϕ_i is the fluence at T_i. This relation, applied to the two cases just mentioned, gives Q = 0.23 eV, slightly larger than the accepted range of 0.02 to 0.2 eV for in-plane diffusion [13] and similar to the interstitial-vacancy repulsion barrier [10]. Obtaining a single value for Q suggests that the nature of the damage is similar in both cases (at least for the flux employed and up to the implantation temperatures investigated here). In room temperature implanted specimens, no evidence of interstitial loops was found by transmission electron microscopy [14]. But interstitials may still be clustered into small groups [11]. Clustering, recombination with vacancies and migration toward the surface, all of which are thermally activated processes, determine the residual interstitial population.

Step-wise annealing was performed on samples implanted to fluences of 5×10^{18} and 5×10^{19} ions/m^2. Damage recovery was observed after annealing the specimens that exhibited

well-separated D- and G-lines for the as-implanted condition. As the annealing temperature was increased, a gradual reduction of the 1360 cm^{-1} line intensity and a gradual increase of the 1580 cm^{-1} line intensity occurred, along with narrowing of both bands. After the 1373 K anneal only a slight D-line was detected. In contrast, recovery of the samples implanted to higher doses was much slower, as illustrated in Fig. 7. In this case, only after the highest temperature anneal (1473 K) is clear separation of the D- and G-lines observable.

Specimens annealed directly at a higher temperature (as opposed to the stepwise annealing described above) exhibited a faster recovery. This behavior is illustrated in Fig. 8 for a specimen implanted at 280 K to 5×10^{21} ions/m^2. Annealing this specimen for 1h at 1273 K gives a Raman spectrum similar to that for the highest temperature anneal of Fig. 7. An additional 1 h anneal at 1373 K shows a definite separation into two lines with maxima near 1580 and 1360 cm^{-1}. This result suggests that annealing at lower temperatures allows for evolution of metastable damage structures that require a higher temperature to recover the undamaged graphite structure.

CONCLUSIONS

The main conclusions of this study are as follows:

1. Radiation damage decreases with increasing irradiation temperature. This suggests a diffusion-controlled mechanism of damage buildup. A value of 0.23 eV can be derived for the activation energy of migration of the defect responsible for damage evolution. It is suggested that this defect is the interstitial.
2. Recovery of the damage by thermal annealing depends on the initial state of damage and on the annealing program. Recovery is more efficient with high-temperature direct annealing rather than with step-wise annealing.
3. At a damage level where two distinct Raman lines cannot be further distinguished, damage structures develop which require high temperatures to anneal. Pre-annealing at lower temperatures stabilizes them into metastable microstructures that are more resistant to annealing than those induced by implantation.

ACKNOWLEDGMENTS

This research was sponsored by the Office of Fusion Energy and the Division of Materials Sciences, U.S. Department of Energy, under contract DE-AC05-84OR21400 with Martin Marietta Energy Systems, Inc. The authors are very indebted to Ms. Dorothy Coffey for her capable assistance in SEM and to Dr. B. Kelly for his valuable comments.

REFERENCES

1. F. Tuinstra and J.L. Koenig, J. Chem. Phys. **53**, 1126(1970).
2. B.S. Elman, M.S. Dresselhaus, G. Dresselhaus, E.W. Maby and H. Mazurek, Phys. Rev. B **24**, 1027 (1981).
3. B.S. Elman, M. Shayegan, M.S. Dresselhaus, H. Mazurek and G. Dresselhaus, Phys. Rev. B**25**, 4412 (1982).
4. T. Tanabe, S. Muto, Y. Gotoh and K. Niwase, J. Nucl. Mater. **175**, 258 (1990).
5. K. Nakamura and M. Kitajima, Appl. Phys. Lett. **59**, 1550 (1991).
6. B.S. Elman, M. Hom, E.W. Maby and M.S. Dresselhaus, MRS Proc Symposium, **20**, 341 (1983).
7. K. Niwase and T. Tanabe, Proc. Intl. Symp. Materials Chemistry in Nuclear Environments, March 1992, Tsukuba - Japan, pp. 437-447.
8. D.S. Knight and W.B. White, J. Mater. Res. **4**, 385 (1989).
9. B.K. Annis, D.F. Pedraza and S.P. Withrow, "Topographical Changes Induced by High Dose Carbon-implantation of Graphite," to be published.
10. a. J.H.W. Simmons, Radiation Damage in Graphite, Pergamon Press (1965); b. B.T. Kelly, Physics of Graphite, Applied Science Publishers (1981).
11. J. Koike and D.F. Pedraza, to be published with the Proc. Intl. Conf. on Beam Processing of Advanced Materials (ASM, Chicago, 1992).
12. J.F. Ziegler, J.P. Biersack and U. Littmark, The Stopping and Range of Ions in Solids, Vol. 1, ed. J.F. Ziegler (Pergamon Press, 1985)
13. P.A. Thrower and R.M. Mayer, Phys. Stat. Sol. (a) **47**, 11 (1978).
14. E.A. Kenik, D.F. Pedraza and S.P. Withrow, to be published.

DISCLAIMER

This report was prepared as an account of work sponsored by an agency of the United States Government. Neither the United States Government nor any agency thereof, nor any of their employees, makes any warranty, express or implied, or assumes any legal liability or responsibility for the accuracy, completeness, or usefulness of any information, apparatus, product, or process disclosed, or represents that its use would not infringe privately owned rights. Reference herein to any specific commercial product, process, or service by trade name, trademark, manufacturer, or otherwise does not necessarily constitute or imply its endorsement, recommendation, or favoring by the United States Government or any agency thereof. The views and opinions of authors expressed herein do not necessarily state or reflect those of the United States Government or any agency thereof.

DATE
FILMED
10/13/94

END